OPEN ACCESS
IOP Publishing | Bureau International des Poids et Mesures Metrologia
Metrologia **60** (2023) 055010 (7pp) https://doi.org/10.1088/1681-7575/acf5f0

Internal quantum efficiency of silicon photodetectors at ultraviolet wavelengths

Mikhail Korpusenko[1,*], Anna Vaskuri[1,2], Farshid Manoocheri[1] and Erkki Ikonen[1,3]

[1] Metrology Research Institute, Aalto University, Espoo, Finland
[2] CERN, Geneva, Switzerland
[3] VTT MIKES, Espoo, Finland

E-mail: mikhail.korpusenko@aalto.fi

Received 2 June 2023, revised 17 August 2023
Accepted for publication 1 September 2023
Published 14 September 2023

Abstract

We determine experimentally the internal quantum efficiency of a 3-element trap detector made of Hamamatsu S1337 photodiodes and of a predictable quantum efficient detector (PQED) over the wavelength range of 250–500 nm using an electrically calibrated pyroelectric radiometer as reference detector. The PQED is made of specially designed induced junction photodiodes, whose charge-carrier recombination losses are minimized. The determined internal quantum efficiency of PQED is always 1 or larger, whereas the 3-element trap detector has internal quantum efficiency smaller than 1 in the spectral range of 330–450 nm. This finding demonstrates the advantages of PQED photodiodes for studying the quantum yield due to impact ionization by charge carriers in the silicon lattice. For this purpose, we develop an extrapolation model for the charge-carrier recombination losses of the PQED, which allows us to separate the quantum yield from the measured internal quantum efficiency. Measurements of PQED spectral responsivity thus allow to determine the quantum yield in silicon, which can be further used for quantifying the charge-carrier recombination losses in the 3-element trap detector. Numerical values of the latter are from 6% to 2% in the spectral range from 250 nm to 380 nm. Finally, our results are encouraging for the aim of developing the PQED to a primary detector standard also at ultraviolet wavelengths.

Keywords: silicon photodiode, induced junction, quantum yield, recombination losses, ultraviolet responsivity, predictable quantum efficient detector

(Some figures may appear in colour only in the online journal)

1. Introduction

Silicon photodiodes are widely used to measure optical power in both research work and applications. The ultraviolet (UV) wavelength range is demanding for accurate optical power measurements because of lack of convenient reference detectors to be used as working standards. An often used working standard at National Metrology Institutes is the 3-element trap detector constructed of commercially available Hamamatsu photodiodes [1–4]. However, the responsivity of those detectors shows significant temporal aging, especially at UV wavelengths [4, 5]. Another alternative is the predictable quantum efficient detector (PQED), whose properties at UV have not yet been much tested, but which has shown excellent performance even as a primary standard at visible wavelengths [6–10].

* Author to whom any correspondence should be addressed.

The properties of the 3-element trap detector and PQED can be characterized relative to an ideal quantum detector which converts each incident photon to a measurable signal. For a silicon photodiode this means that an ideal quantum detector converts each absorbed photon to exactly one electron-hole pair to produce photocurrent in an external circuit. Such feature leads to a simple expression for the ideal spectral responsivity $R_0(\lambda) = e\lambda/hc$ in units of A/W as a function of vacuum wavelength λ, where *e, h* and *c* are fundamental constants. For the spectral responsivity of a real silicon detector, correction factors can be written in the form

$$R(\lambda) = R_0(\lambda)(1-\rho(\lambda))(1-\delta(\lambda))(1+g(\lambda)), \quad (1)$$

where parameters $\rho(\lambda)$ and $\delta(\lambda)$ describe the losses by spectral reflectance and recombination of charge carriers, respectively, and $1 + g(\lambda)$ is the quantum yield, which may produce more than one electron-hole pair per absorbed photon. In general, numerical values of $\rho(\lambda)$ and $\delta(\lambda)$ can be small for trap detectors and for good quality photodiodes even at UV wavelengths, whereas it is known that quantum yield can reach values much above 1 for vacuum UV [11]: high energy photons can produce electron-hole pairs which have sufficient energy to produce secondary charge carriers via impact ionization. It is of interest to study theoretically the asymptotic form of $1 + g(\lambda)$ at low photon energies as presented in [12].

The responsivity ratio $R(\lambda)/R_0(\lambda)$, which is equal to the product of the three factors in parentheses in equation (1), is called external quantum efficiency of the detector. In the internal quantum efficiency,

$$\eta_i(\lambda) = (1-\delta(\lambda))(1+g(\lambda)), \quad (2)$$

the effect of detector reflectance is corrected from the responsivity ratio.

In measurements of single photodiodes accurate determination of responsivity is complicated because of significant reflectance losses, which can be more than 50% at UV with a strong dependence on the angle of incidence [13]. In a trap detector, the specularly reflected component from a photodiode is collected by another photodiode of the detector reducing the reflectance correction $\rho(\lambda)$ of equation (1). Recombination losses of equation (1) can be traced indirectly by comparison of responsivity against cryogenic radiometer [14–16] or directly by exploitation of simulation models based on fundamental photodiode parameters and auxiliary measurements [10, 17, 18]. In the visible wavelength range quantum yield is often neglected which allows determination of recombination losses from the responsivity measured by cryogenic radiometer and reflectance of the detector [19]. However, for the UV range separation of the components of internal quantum efficiency $\eta_i(\lambda)$ to recombination losses and quantum yield is difficult without additional information.

In this paper, we determine experimentally the internal quantum efficiency $\eta_i(\lambda)$ of a 3-element trap detector and of PQED over the wavelength range of 250–550 nm using an electrically calibrated pyroelectric radiometer (ECPR) as reference detector. A significant finding is that $\eta_i(\lambda)$ of PQED is always 1 or larger, whereas for 3-element trap detector $\eta_i(\lambda) < 1$ at wavelengths around 370 nm. The charge-carrier recombination losses in the 3-element trap detector dominate over quantum yield, in contrast to results of the PQED. Furthermore, we present an extrapolation model for the charge-carrier recombination losses of the PQED, which allows us to separate the quantum yield from measured internal quantum efficiency. It is concluded that measurements of PQED spectral responsivity give access to quantitatively determine the quantum yield in silicon lattice caused by impact ionization at most of UV and short visible wavelengths. Comparison with the results of a theoretical calculation of quantum yield is encouraging for the aim of developing the PQED to a primary detector standard also at UV wavelengths.

2. Detectors under test

Figure 1 describes the silicon photodetectors used in this study. The 3-element trap detector is made of windowless Hamamatsu S1337 silicon photodiodes of 10 mm × 10 mm active area. The planes of incidence of each photodiode are perpendicular to each other which makes the responsivity of the detector independent on the polarization state of incident radiation. The PQED is based on two induced-junction silicon photodiodes of active area 22 mm × 11 mm in a wedge trap configuration. Several specular reflections take place after which a small fraction of incident light escapes via the entrance aperture. The PQED is sensitive to the polarization of incident light, but this is not a serious limitation because the most accurate spectral responsivity measurements are in any case carried out with plane polarized collimated laser beams. There is a thin SiO_2 layer on the surface of both Hamamatsu and PQED photodiodes. In the former case the thickness is about 30 nm [13]. For the PQED, the SiO_2 layer thickness is 300 nm on the first photodiode and 200 nm on the second photodiode [6].

Measured and calculated reflectances of single photodiodes [13] and trap detectors [6, 8] are generally in good agreement. Above 300 nm wavelength, the agreement is within 1% of the reflectance value [13]. Thus, for this work it is sufficient to use detector reflectances calculated on the basis of geometry (figure 1) and (complex) refractive indices of SiO_2 [20], of undoped silicon [21] for PQED, and of doped silicon [22] for Hamamatsu photodiodes, used also in [13]. Results of the calculations are shown in figure 2. If the refractive indices of [21] would be used instead of [22] for the 3-element trap detector, the reflectance losses would increase by 0.002–0.003 in the range 260–295 nm, and much less at other wavelengths. For PQED, reflectance losses are below 0.01% in mid visible range and stay below 0.5% down to 320 nm wavelength, while for the 3-element trap detector the reflectance losses are between 0.5% and 3% in the whole spectral range above 320 nm. Both types of detectors have a reflectance peak at 370 nm, whereas

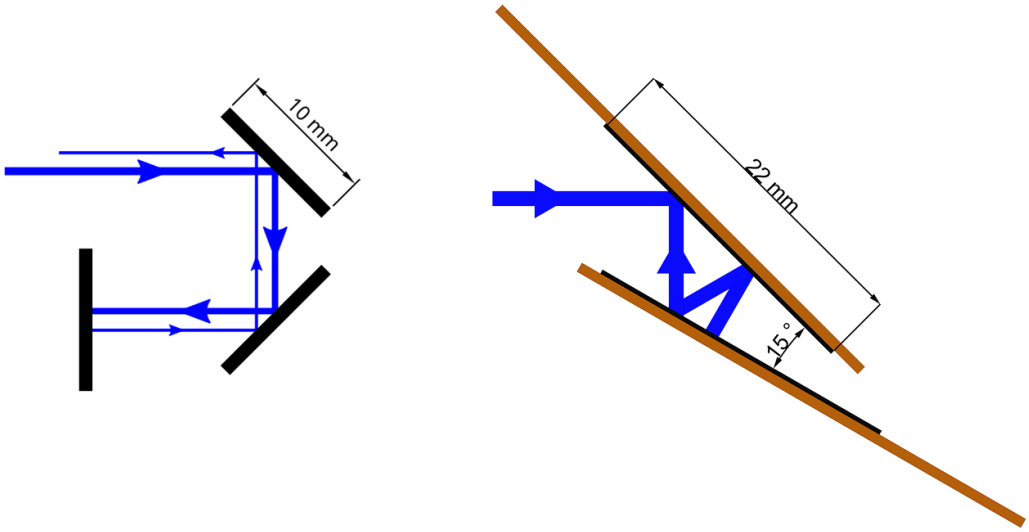

Figure 1. Schematic structure of 3-element trap detector (left) and 2-element PQED with seven reflections (right). The five reflections of 3-element trap detector are usually arranged in three dimensions so that the responsivity becomes independent on the polarization state of incident light, whereas the responsivity of PQED is sensitive to polarization.

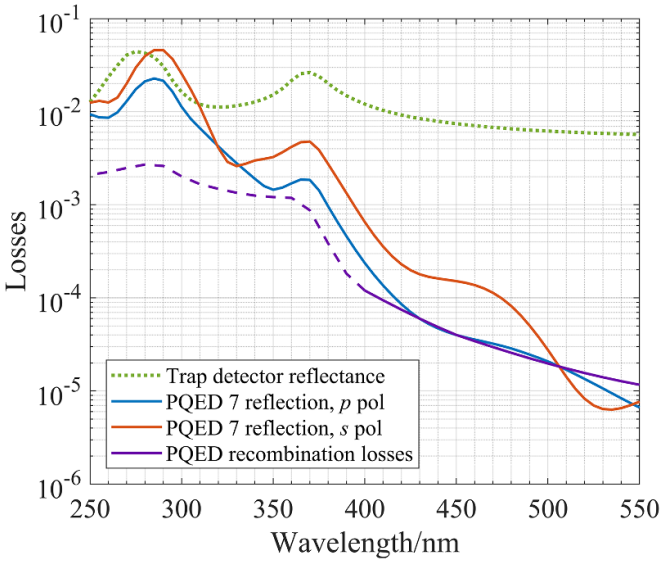

Figure 2. Calculated reflectance losses of polarization insensitive 3-element trap detector (green dotted line) and of PQED with *p* polarized (blue line) and *s* polarized (orange line) incident light. The continuous purple line shows simulated charge-carrier recombination losses in PQED photodiodes from [10] and the dashed purple line indicates an extrapolation of the recombination losses, based on the penetration depth of UV and visible light in silicon.

the peaks at shorter wavelengths are at 275 nm and at 285 nm for the 3-element trap detector and PQED, respectively. This difference is caused by different SiO_2 layer thicknesses.

Figure 2 also shows charge-carrier recombination losses of PQED photodiodes in the spectral range from 400 nm to 550 nm, calculated by a 3D simulation model [10]. The contribution by surface recombination dominates in this spectral range as compared with bulk recombination losses. Surface effects become more dominant at short wavelengths because the penetration depth in silicon is about 1000 nm, 100 nm and 10 nm at the wavelengths of 500 nm, 400 nm and 360 nm, respectively [21]. The surface recombination losses increase by an order of magnitude when the wavelength changes from 500 nm to 400 nm when also the penetration depth changes by an order of magnitude. In the extrapolated curve of figure 2, recombination losses and penetration depth change by another order of magnitude from 400 nm to 360 nm. At even shorter wavelengths, the penetration depth stays constant within a factor of two between 360 nm and 250 nm, which leads to a conclusion on similar weak wavelength dependence also for the extrapolated charge-carrier losses in this spectral range.

The true charge-carrier recombination losses at UV wavelengths may deviate by a factor of two from the extrapolated values in figure 2. Nevertheless, the recombination losses of PQED photodiodes stay much below the level of 1% and also much below the reflectance losses of PQED for most of the UV wavelengths. The situation is completely different with the Hamamatsu photodiodes used for the 3-element trap detector. Their charge-carrier recombination losses are expected to be of the order of 1% at UV wavelengths, but there is no theoretical description available for a more accurate estimate. Moreover, stability studies of silicon photodiodes indicate that the mechanisms for charge-carrier recombination losses may be different in Hamamatsu photodiodes and in PQED photodiodes at short visible and UV wavelengths [5].

3. Measurement setup

The measurement setup (figure 3) consists of a xenon lamp, monochromator, broadband wire-grid polarizer for producing light with different polarization states, half-wave plate, parabolic mirror to image the exit slit of the monochromator on the radiometers, monitor detector, and reference ECPR LaserProbe Rs-5900. Our results of CCPR-K2.c key comparison indicate that the spectral flatness of the responsivity of

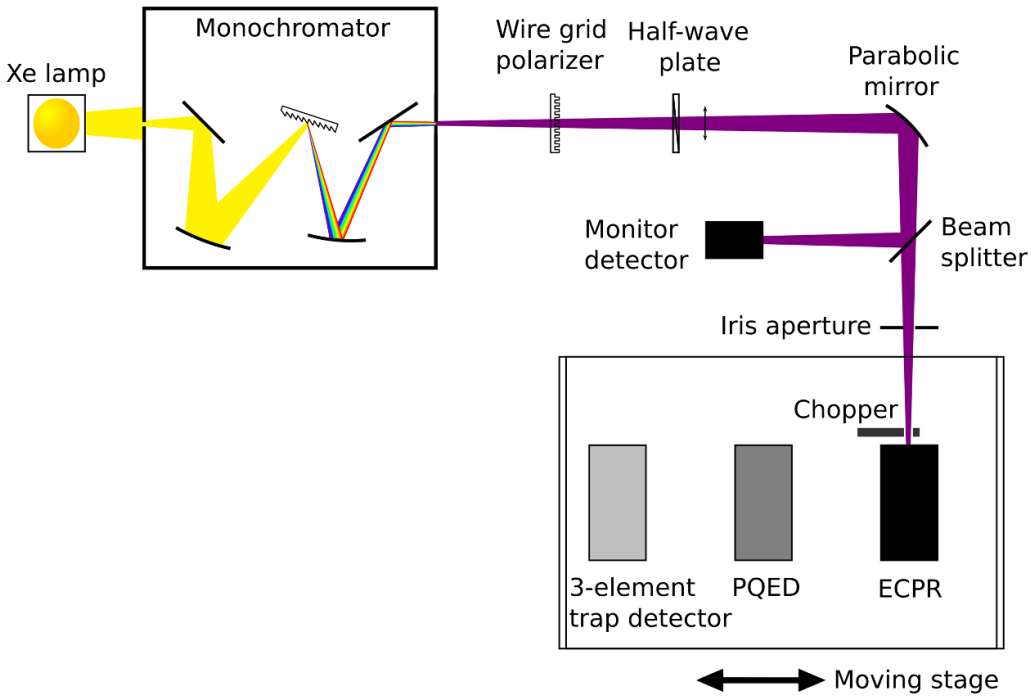

Figure 3. Measurement setup.

ECPR is within 0.5% in the range 250–400 nm [23]. The detectors under test are PQED and 3-element trap detector made of Hamamatsu photodiodes. A reverse bias voltage of 5 V was used with the PQED, while the 3-element trap detector was used unbiased. As the Brewster window was not used with PQED, dry nitrogen gas flow through the PQED was used to protect the PQED photodiodes from contamination by particles in the normal laboratory air [24].

Comparison responsivity measurements were carried out with ECPR against PQED and trap detector over the spectral range of 250–550 nm. The software executed the comparison measurement in such a way that first the measurement wavelength was selected and then the moving stage was successively changed to a position for recording the signal either from the ECPR, PQED, or 3-element trap detector. Signal from the monitor detector was used to correct for intensity drifts of the light source. The software repeated the measurement of each detector signal several times at each wavelength to reduce noise by averaging.

4. Internal quantum efficiency

Photocurrent signal from the test detectors was divided by the optical power obtained from the ECPR, to determine the measured spectral responsivity $R(\lambda)$ of equation (1). Results are shown in figure 4 for the 3-element trap detector and PQED, where the expanded measurement uncertainty is approximately 1% between 275 nm and 550 nm while it is somewhat larger below 275 nm because of low signal level of ECPR. It is seen that the responsivity of PQED is larger than that of the 3-element trap detector. As compared with the responsivity of ideal quantum detector, PQED responsivity values are, on the average, on the straight line or above it, whereas the responsivity of the 3-element trap detector is below the ideal responsivity at short visible wavelengths. At short UV wavelengths the measured spectral responsivity of both detectors is mostly above the ideal responsivity because of increased quantum yield. The responsivity of PQED for *s*-polarized light is lower than for *p*-polarized light at wavelengths from 250 nm to 310 nm, because reflectance of the former is larger in that spectral range as seen in figure 2.

The ratio of measured and ideal responsivity can be used for determination of the internal quantum efficiency by correcting for the effect of detector reflectance, factor $1 - \rho(\lambda)$ from equation (1) and figure 2. Figure 5 shows the results for the internal quantum efficiency $\eta_i(\lambda)$ of the 3-element trap detector and PQED. It should be noted that the values of $\eta_i(\lambda)$ of PQED are approximately the same for the different polarization states of incident radiation, as it should be. Enhanced $\eta_i(\lambda)$ values are observed around 285 nm and 370 nm wavelengths, especially in the PQED data. The peak at 370 nm corresponds to direct transition at Γ point of Brillouin zone [25] and is detectable for PQED but not for the trap because the contribution of recombination loss is larger than that of quantum yield around 370 nm. The peak at 285 nm due to direct bandgap transition in silicon at X point [25] is observable for both detectors.

The extrapolated charge-carrier recombination loss $\delta(\lambda)$ in figure 2 and its uncertainty are sufficiently small for PQED so that the quantum yield $1 + g(\lambda)$ can be extracted from $\eta_i(\lambda)$ after division by $1 - \delta(\lambda)$. The result is shown in figure 6, which also depicts a theoretical prediction for the quantum yield with [12]

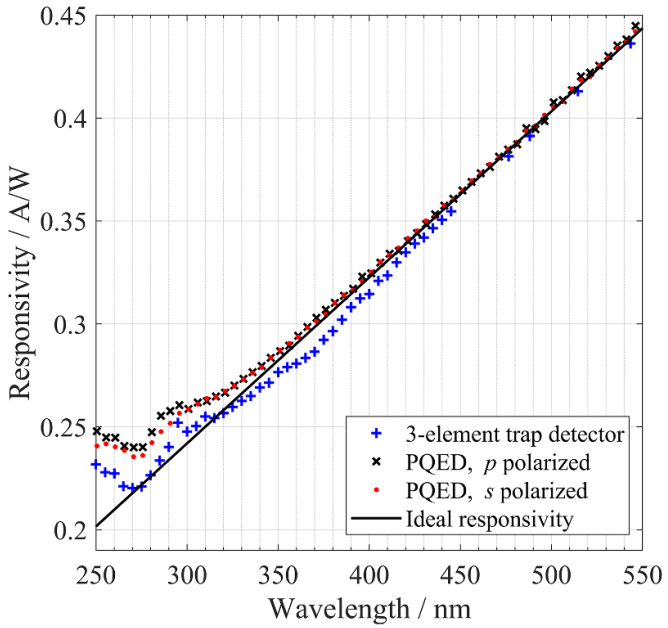

Figure 4. Measured responsivity of 3-element polarization insensitive trap detector and of PQED with *p*-polarized (black crosses) and *s*-polarized (red dots) incident light. Straight black line indicates the ideal responsivity of a quantum detector, where each incident photon is converted to exactly one electron-hole pair.

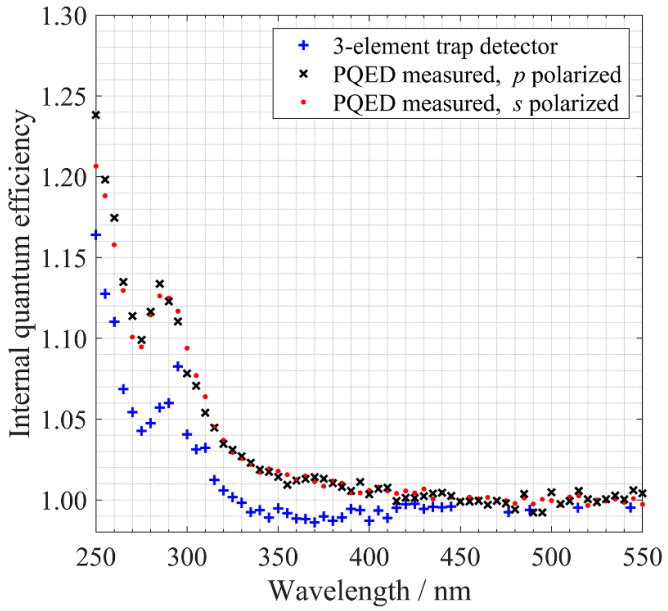

Figure 5. Measured internal quantum efficiency of 3-element polarization insensitive trap detector and of PQED with *p*-polarized (black crosses) and *s*-polarized (red dots) incident light.

$$g(\lambda) = \left[1 + A_1\left(\frac{hc}{\lambda} - E_g - E_{ph} - \Delta E\right)^{1/2} \Big/ \times \left(\frac{hc}{\lambda} - 2E_g - \Delta E\right)^{7/2}\right]^{-1} \quad (3)$$

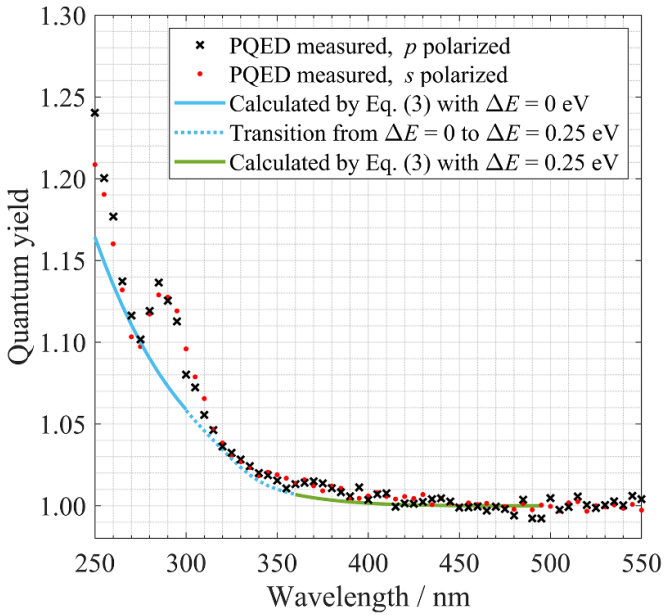

Figure 6. Measured quantum yield of PQED with *p*-polarized (black crosses) and *s*-polarized (red dots) incident light. Solid line is calculated by equation (3) with $\Delta E = 0$ for $\lambda < 300$ nm (blue) and $\Delta E = 0.25$ eV for $\lambda > 360$ nm (green). Blue dotted line represents the transition from $\Delta E = 0$ to $\Delta E = 0.25$ eV.

where $A_1 = 105A/(2\pi) = 86.9$ eV^3 is the constant derived in [26], $E_g = 1.12$ eV is the indirect energy gap in silicon at room temperature, $E_{ph} = 0.063$ eV is the energy of optical phonon in silicon [27] and ΔE is an energy shift, which is zero below 300 nm wavelength and 0.25 eV above 360 nm. In the wavelength range of 300–360 nm, there is a shift of the value of ΔE from 0 eV to 0.25 eV. The relative deviation of $g(\lambda)$ between calculated and measured results is small, except for the peaks of enhanced impact ionization at 285 nm and 370 nm. Accounting for these peaks calls for an improved calculation of the quantum yield considering the detailed energy band structure in silicon lattice.

Several simplifying assumptions were made in deriving equation (3) [12, 26, 28]. Electrons and holes taking part in impact ionization are described by the density of states of free particles and they are assumed to contribute equally. In addition, all available energy is assumed to be taken either by the electron or the hole and the considered energy dissipation processes are electron-hole pair creation and emission of optical phonons. Finally, at wavelengths longer than 360 nm the above impact ionization processes appear to have reduced efficiency which can be described by the energy shift $\Delta E = 0.25$ eV in equation (3) [12, 29].

Based on above assumptions, it is concluded that in the spectral ranges where the quantum yield of PQED photodiodes, with very low impurity concentration, is sufficiently described by equation (3), the measured quantum yield of PQED also applies to Hamamatsu photodiodes which have much higher impurity doping level. In photodiodes with

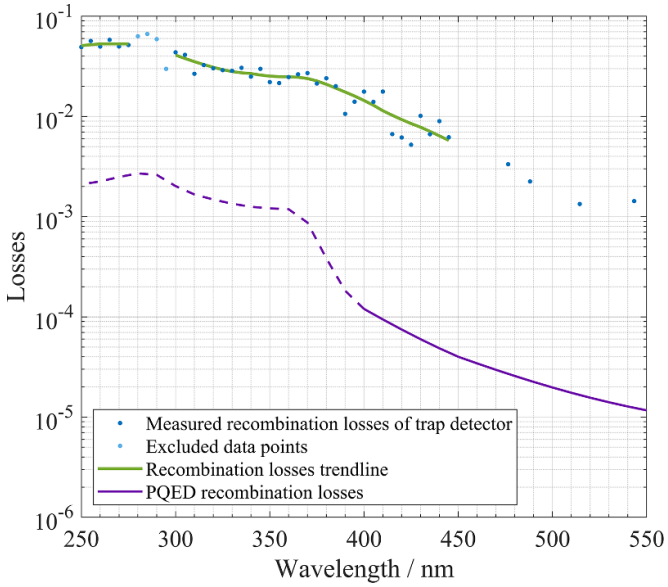

Figure 7. Estimated charge-carrier recombination losses in the Hamamatsu photodiodes of the 3-element trap detector (blue dots). Data points at the range of 280–295 nm are not used for calculation of recombination losses because of insufficient quantum yield estimate. The trendline follows the data within deviations of 0.01, corresponding to the relative expanded measurement uncertainty of 1% in spectral responsivity. For comparison, also simulated/extrapolated charge-carrier recombination losses in the PQED photodiodes from figure 2 are shown.

impurity doping, the added atoms are mostly substituting silicon atoms in the crystal lattice. Even at a heavy doping level of 10^{19} cm^{-3}, there are 5000 silicon atoms for each impurity atom. After photon absorption, most charge carriers are thus created in an environment of a regular silicon crystal lattice, suggesting that the impact ionization capabilities of the charge carriers are similar in undoped and heavily doped lattices up to 10^{19} cm^{-3}.

For the Hamamatsu photodiodes a reliable estimate of charge-carrier recombination losses is not available at UV wavelengths and thus a similar quantum yield estimate as for PQED photodiodes cannot be made. Instead, the quantum yield obtained from PQED photodiodes can be used to estimate the charge-carrier recombination losses of Hamamatsu photodiodes by dividing $\eta_i(\lambda)$ of the 3-element trap detector of figure 5 with the experimental quantum yield of figure 6. The outcome is shown in figure 7, where the data points at the range of 280–295 nm are excluded from calculation of the recombination loss of the trap detector, because at these wavelengths the difference of quantum yield of PQED and Hamamatsu photodiodes can be up to 0.03, as seen from the difference of peak heights in figure 5. For the other peak at 370 nm, the data can be included in the analysis because the relative quantum yield correction to internal quantum efficiency is much smaller than at 285 nm. A continuous trendline has been included in figure 7 as a guide to the eye, without any connection to physical recombination loss models.

The charge-carrier recombination losses in the Hamamatsu photodiodes at the UV wavelengths are between 2% and 6% and thus much larger than those of the PQED photodiodes (figure 7). Induced junction photodiodes have very low impurity concentration unlike conventional p-n junction photodiodes which enhances bulk recombination and measured losses of the 3-element trap detector as compared to the PQED. There is only weak dependence of the recombination losses on the wavelength, in agreement with the extrapolation made for the PQED photodiodes. Furthermore, there are no residual features of the peaks in the reflectance curve in the recombination losses, which indicates that the reflectance and quantum yield corrections have worked well.

5. Conclusions

We have measured spectral responsivities of induced junction photodiodes of PQED and Hamamatsu photodiodes of 3-element trap detector against ECPR to determine the internal quantum efficiency of the photodiodes in the UV spectral range. There is a fundamental difference in the charge-carrier recombination losses of these two types of photodiodes, which allowed the quantum yield to be determined only for the induced junction photodiodes. Our calculated result for the quantum yield has very good agreement with results of PQED measurements at wavelengths where direct bandgap transitions in silicon do not affect impact ionization rate and, thus, quantum gain. Hamamatsu photodiodes were assumed to have the same quantum yield as PQED photodiodes. This allowed to determine the charge-carrier recombination losses of Hamamatsu photodiodes from their experimentally determined internal quantum efficiency for most of the studied spectral range.

Responsivity measurements of room-temperature PQED relative to absolute cryogenic radiometers in the wavelength range from 476 nm to 800 nm indicate that PQED can be used as a primary standard of optical power with a relative expanded uncertainty of about 0.01% [5, 7]. Even lower uncertainties can be achieved in that spectral range with the help of auxiliary relative measurements and advanced simulations of the charge-carrier recombination losses [10]. Operation and maintenance of a set of PQEDs is much easier than the use of cryogenic radiometers. It would thus be highly preferable that PQED could be exploited as a primary standard for optical power measurements over the whole spectral range of silicon photodetectors. Our results provide a major step towards that direction by validating a general dependence of internal quantum efficiency and quantum yield in silicon at UV wavelengths.

Acknowledgments

Projects 18SIB10 Chipscale and 22IEM06 ScaleUp leading to this publication have received funding from the EMPIR program and from the European Partnership on Metrology, respectively, co-financed by the participating states and the European Union's Horizon 2020 and Horizon Europe research and innovation programmes. We also acknowledge support

by the Academy of Finland Flagship Programme, Photonics Research and Innovation (PREIN), Decision Number 320167.

ORCID iDs

Mikhail Korpusenko https://orcid.org/0000-0003-4329-1007
Anna Vaskuri https://orcid.org/0000-0003-1246-4550
Erkki Ikonen https://orcid.org/0000-0001-6444-5330

References

[1] Fox N P 1991 Trap detectors and their properties *Metrologia* **28** 197–202
[2] Houston J M, Cromer C L, Hardis J E and Larason T C 1993 Comparison of the NIST high accuracy cryogenic radiometer and the NIST scale of detector spectral response *Metrologia* **30** 285–90
[3] Kärhä P, Toivanen P, Manoochehri F and Ikonen E 1997 Development of a detector-based absolute spectral irradiance scale in the 380–900-nm spectral range *Appl. Opt.* **36** 8909
[4] Werner L, Fischer J, Johannsen U and Hartmann J 2000 Accurate determination of the spectral responsivity of silicon trap detectors between 238 nm and 1015 nm using a laser-based cryogenic radiometer *Metrologia* **37** 279–84
[5] Porrovecchio G, Linke U, Smid M, Gran J, Ikonen E and Werner L 2022 Long-term spectral responsivity stability of predictable quantum efficient detectors *Metrologia* **59** 065008
[6] Sildoja M, Manoocheri F, Merimaa M, Ikonen E, Müller I, Werner L, Gran J, Kübarsepp T, Smîd M and Rastello M L 2013 Predictable quantum efficient detector: I. Photodiodes and predicted responsivity *Metrologia* **50** 385–94
[7] Müller I *et al* 2013 Predictable quantum efficient detector: II. Characterization and confirmed responsivity *Metrologia* **50** 395–401
[8] Dönsberg T, Sildoja M, Manoocheri F, Merimaa M, Petroff L and Ikonen E 2014 A primary standard of optical power based on induced-junction silicon photodiodes operated at room temperature *Metrologia* **51** 197–202
[9] Koybasi O *et al* 2021 High performance predictable quantum efficient detector based on induced-junction photodiodes passivated with SiO_2/SiNx *Sensors* **21** 7807
[10] Tran T, Porrovecchio G, Smid M, Ikonen E, Dönsberg T and Gran J 2022 Determination of the responsivity of a predictable quantum efficient detector over a wide spectral range based on a 3D model of charge carrier recombination losses *Metrologia* **59** 045012
[11] Scholze F, Henneken H, Kuschnerus P, Rabus H, Richter M and Ulm G 2000 Determination of the electron–hole pair creation energy for semiconductors from the spectral responsivity of photodiodes *Nucl. Instrum. Methods Phys. Res.* A **439** 208–15
[12] Korpusenko M, Vaskuri A, Manoocheri F and Ikonen E 2023 Impact ionization in silicon at low charge-carrier energies *AIP Adv.* **13** 085119
[13] Haapalinna A, Kärhä P and Ikonen E 1998 Spectral reflectance of silicon photodiodes *Appl. Opt.* **37** 729
[14] Martin J E, Fox N P and Key P J 1985 A cryogenic radiometer for absolute radiometric measurements *Metrologia* **21** 147–55
[15] Varpula T, Seppa H and Saari J-M 1989 Optical power calibrator based on a stabilized green He-Ne laser and a cryogenic absolute radiometer *IEEE Trans. Instrum. Meas.* **38** 558–64
[16] Foukal P V, Hoyt C, Kochling H and Miller P 1990 Cryogenic absolute radiometers as laboratory irradiance standards, remote sensing detectors, and pyroheliometers *Appl. Opt.* **29** 988–93
[17] Gran J, Kübarsepp T, Sildoja M, Manoocheri F, Ikonen E and Müller I 2012 Simulations of a predictable quantum efficient detector with PC1D *Metrologia* **49** S130–4
[18] Dönsberg T *et al* 2017 Predictable quantum efficient detector based on *n* -type silicon photodiodes *Metrologia* **54** 821–36
[19] Manoocheri F, Sildoja M, Dönsberg T, Merimaa M and Ikonen E 2014 Low-loss photon-to-electron conversion *Opt. Rev.* **21** 320–4
[20] Gao L, Lemarchand F and Lequime M 2013 Refractive index determination of SiO_2 layer in the UV/Vis/NIR range: spectrophotometric reverse engineering on single and bi-layer designs *J. Eur. Opt. Soc.* **8** 13010
[21] Green M A 2008 Self-consistent optical parameters of intrinsic silicon at 300K including temperature coefficients *Sol. Energy Mater. Sol. Cells* **92** 1305–10
[22] Jellison G E 1992 Optical functions of silicon determined by two-channel polarization modulation ellipsometry *Opt. Mater.* **1** 41–47
[23] Werner L 2014 Final report on the key comparison CCPR-K2.c-2003: spectral responsivity in the range of 200 nm to 400 nm *Metrologia* **51** 02002
[24] Askola J, Maham K, Kärhä P and Ikonen E 2021 Increased detector response in optical overfilled measurements due to gas lens formation by nitrogen flow through the entrance aperture *Metrologia* **58** 055008
[25] Kolodinski S, Werner J H, Wittchen T and Queisser H J 1993 Quantum efficiencies exceeding unity due to impact ionization in silicon solar cells *Appl. Phys. Lett.* **63** 2405–7
[26] Alig R C, Bloom S and Struck C W 1980 Scattering by ionization and phonon emission in semiconductors *Phys. Rev.* B **22** 5565–82
[27] Jacoboni C and Reggiani L 1983 The Monte Carlo method for the solution of charge transport in semiconductors with applications to covalent materials *Rev. Mod. Phys.* **55** 645–705
[28] Ramanathan K and Kurinsky N 2020 Ionization yield in silicon for eV-scale electron-recoil processes *Phys. Rev.* D **102** 063026
[29] Wolf M, Brendel R, Werner J H and Queisser H J 1998 Solar cell efficiency and carrier multiplication in $Si_{1-x}Ge_x$ alloys *J. Appl. Phys.* **83** 4213–21